Journal of Applied Pharmaceutical Science Vol. 15(03), pp 174-182, March, 2025
Available online at http://www.japsonline.com
DOI: 10.7324/JAPS.2025.202888
ISSN 2231-3354

Quality by design approach assisted development and optimization of Chitosan–Vildagliptin nanoparticles using a simple desolvation technique

Anand Shripal Ammanage[1,2], Vinayak Shivamurthi Mastiholimath[2*]

[1]Department of Pharmaceutics, KLES's College of Pharmacy Nipani, Rajiv Gandhi University of Health Sciences Bengaluru, Bengaluru, India.
[2]Department of Pharmaceutical Quality Assurance, KLE College of Pharmacy Belagavi, KLE Academy of Higher Education and Research, Belagavi, India.

ARTICLE HISTORY

Received on: 24/09/2024
Accepted on: 25/12/2024
Available Online: 05/02/2025

Key words:
Chitosan, vildagliptin, quality by design, diabetes mellitus, desolvation method.

ABSTRACT

Type 2 diabetes mellitus is a major metabolic condition that poses a serious risk and a significant public health concern worldwide. Vildagliptin is a new class of antidiabetic drugs used to treat type 2 diabetes mellitus. In the current work, Chitosan-Vildagliptin nanoparticles (CS-VLD NPs) were developed by simple desolvation technique. A 3^2 factorial design and response surface methodology were used for optimization. The prepared nanoparticles underwent characterization to determine their particle size (PS), polydispersity index (PDI), entrapment efficiency (EE), FTIR, transmission electron microscopy (TEM), *in vitro* drug release, and release kinetics. A 3-month accelerated stability study was performed for the optimized formulation (N6). The PDI value of CS-VLD NPs was varied from 0.24 ± 0.025 to 0.39 ± 0.037, while the PSs were ranged from 118.24 ± 2.26 nm to 232.84 ± 6.79 nm. The EE values were varied from 26.54 ± 3.61 to 51.57% ± 1.52%. FTIR study had shown the compatibility of drug and polymer. TEM images were shown spherical-shaped nanoparticles. During the *in vitro* drug release study, sustained drug release was found up to 24 hours, followed by Higuchi kinetics. During the stability study, the optimized (N6) formulation proved its stability. The study concludes that the developed CS-VLD NPs may be a more effective approach than conventional drug delivery for the sustained release of Vildagliptin in the treatment of diabetes mellitus.

INTRODUCTION

Type 2 diabetes represents a significant metabolic disorder, posing a substantial threat as a major global health concern. This condition exerts direct or indirect adverse impacts on the overall quality of life [1]. The condition is largely caused by diminished sensitivity to insulin or insulin resistance, and the progressive degeneration of pancreatic beta cells [2]. Glucose absorption decreases when insulin sensitivity is reduced, which results in a diminished cellular response to glucose. Thus, hyperglycemia and the harmful consequences of glucotoxicity arise [3]. Diabetes was the cause of 1.6 million deaths in 2016 alone. Predictions state that there will be an increase in the number of diabetes cases, with estimates of 643 million by 2030 and 783 million by 2045 [4].

Metformin and sulfonylureas are frequently prescribed drugs for managing Type 2 Diabetes Mellitus. However, there is a possibility that these oral hypoglycemic agents will cause side effects such as hypoglycemia, liver damage, pancreatitis, and stomach pain. Therefore, there is a critical need to develop innovative and effective anti-hyperglycemic drugs that can reach the appropriate glycemic levels without increasing the risk of hypoglycemia. Treatment for type II diabetes has advanced significantly with the use of incretin hormones. Notably, glucose-dependent insulinotropic peptide (GIP) and glucagon-like peptide-1 (GLP-1) are two novel, potentially effective approaches to treat type 2 diabetes [5].

Significantly, the very short half-lives of GLP-1 and GIP are caused by the enzyme dipeptidyl peptidase-4 (DPP-

*Corresponding Author
Vinayak Shivamurthi Mastiholimath, Department of Pharmaceutical Quality Assurance, KLE College of Pharmacy Belagavi, KLE Academy of Higher Education and Research, Belagavi, India.
E-mail: mastiholimath @ rediffmail.com

4). Thus, it is considered that inhibiting DPP-4 is a suitable approach for treating type 2 diabetes [6].

Vildagliptin is an inhibitor of the DPP-4 enzyme that has been studied extensively in the treatment of diabetes. Its molecular interactions with the DPP-4 enzyme have greatly advanced our understanding of this drug [7].

However, its glucose-lowering effects are transient due to a short half-life of 2–3 hours. As a result, diabetic patients are strongly advised to strictly adhere to the prescribed dosing schedule to maintain its efficacy [8].

Polymeric nanoparticles are pivotal in augmenting the efficacy of therapeutic agents by prolonging their circulation half-lives and diminishing phagocytic uptake and inactivation. These nanoparticles are prepared from synthetic or semi-synthetic polymeric blocks, incorporating biodegradable polymers to optimize tissue compatibility while minimizing cytotoxicity. Chitosan, a naturally occurring polymer, is produced by deacetylating chitin. It is nontoxic, biocompatible, biodegradable, and biologically safe [9].

Chitosan has been recognized as one of the most effective biopolymers for developing formulations that provide sustained ocular delivery [10]. Furthermore, some other research works have demonstrated that Chitosan nanocarriers interact with the ocular mucosa and extend their residence time [11–13]. In oral drug delivery, Chitosan's mucoadhesive properties are essential, as they enable it to stick to the mucosal lining of the gastrointestinal tract, thus enhancing localized drug delivery and absorption. The review by Mohammed *et al.* [14] examines how Chitosan can successfully overcome gastrointestinal barriers, boosting drug absorption and allowing for controlled release. The study highlights the importance of Chitosan's ability to adhere to the intestinal lining, which improves drug absorption and bioavailability [14].

In this instance, we used Chitosan (CS) as the starting material to prepare a typical oral nanoparticles drug delivery system of VLD by desolvation process. To avoid the complexity of the process adopted by earlier mentioned studies, in the current study, Chitosan having low molecular weight was used at three different levels to prepare nanoparticles.

Nowadays, there is an increasing focus on Quality by Design (QbD) as a systematic approach to ensure the quality of the products to accomplish certain goals, such as reduced costs, faster time-to-market, logical controls, and increased efficiency [15]. As QbD is useful in streamlining several processes and producing more stable and effective formulations, its application has grown significantly. Utilizing risk assessment also helps to improve comprehension of important techniques and product limitations [16]. Application of response surface methodology (RSM) and design of experiments (DoEs) is necessary to establish a design space for the input variables in the formulation [17]. DoE and RSM make it possible to collect data efficiently with fewer runs than with standard experimental designs, which change one variable at a time. This combination provides mathematical models that show output responses based on input variables and can be used to analyze response surfaces using linear or quadratic functions. Determining the ideal settings for these input variables becomes crucial to achieving the expected performance of the formulation; in this regard, DoE and RSM are useful techniques [18].

In the present work, an attempt was made to develop Chitosan-loaded Vildagliptin nanoparticles by adopting a simple desolvation technique with QbD concept. The use of natural biodegradable polymers avoids the biocompatibility issue associated with nanoformulations. Furthermore, there is no any requirement for sophisticated equipment for the formulation thus it can be prepared at a small-scale laboratory and can be easily transferred at the production level.

MATERIALS AND METHODS

Materials

Vildagliptin was supplied as a complimentary sample from Ajanta Pharma Ltd. Mumbai, while low molecular weight Chitosan (CS), glutaraldehyde (GA), and acetone were procured from SD Fine Chemicals Ltd. Mumbai. Dialysis membrane (MW of 12 KDa) was brought from HiMedia, Mumbai, India. All other excipients and solvents used in the formulation were of analytical grade.

Preparation of Chitosan-Vildagliptin nanoparticles (CS-VLD NPs)

Vildagliptin-loaded Chitosan nanoparticles were developed using a simple desolvation method with a few small modifications [10]. Briefly, in a 50 ml aqueous acetic acid (2%) solution, various concentrations of CS 200 mg, 400 mg, and 600 mg were dissolved separately and then 100 mg of VLD was added to form a homogeneous solution. Desolvation was then induced by adding acetone drop-by-drop while continuously stirring until a slight permanent turbidity was achieved. Following that, different volumes (50 µl, 100 µl, and 150 µl) of glutaraldehyde (GA) were incorporated as a cross-linking agent, and the solution was stirred overnight at 600 rpm using a mechanical stirrer to facilitate acetone evaporation. The obtained nanoparticles were collected by centrifugation (KUBOTA 7,000, Japan) at 4°C, 20,000 rpm for 1 hour. The sediment was washed with the same conditions in triplicate. A total of nine formulations were prepared and are presented in Table 1.

Statistical experimental design

Pharmaceutical formulations were traditionally developed by adjusting one variable at a time. This method requires an extensive amount of effort and time. Furthermore, it could be difficult to come up with an ideal formulation because the traditional method does not take the combined impacts of independent components into consideration. Thus, using well-established statistical tools like factorial designs is essential to understand the complexity of pharmaceutical compositions. The number of independent variables used in the study will determine how many experiments are required. Table 2 depicts the total factorial experimental design. The amount of GA used and the concentration of CS were the two independent variables that were examined. Three levels (low, medium, and high) of each variable were examined and their effects on two dependent

Table 1. Experimental runs and their observed values of dependent variables.

Runs	Formulation codes	Independent variables		Dependent variables					
				Y_1 (nm)			Y_2 (%)		
		X_1	X_2	Actual	Predicted	Residual	Actual	Predicted	Residual
1	N1	200	50	148.28 ± 2.48	149	−0.7206	26.54 ± 3.61	30.52	−3.98
2	N2	200	100	132.48 ± 4.47	132.83	−0.35	42.18 ± 2.78	38.01	4.17
3	N3	200	150	118.24 ± 2.26	116.67	1.57	43.49 ± 2.64	45.5	−2.01
4	N4	400	50	191.61 ± 4.79	190.88	0.7278	35.69 ± 3.03	34.9	0.7933
5	N5	400	100	176.36 ± 3.60	174.72	1.64	44.64 ± 4.73	42.39	2.25
6	N6	400	150	155.18 ± 3.09	158.55	−3.37	50.45 ± 1.56	49.88	0.5733
7	N7	600	50	232.84 ± 6.79	232.76	0.0761	38.34 ± 3.65	39.28	−0.9367
8	N8	600	100	215.14 ± 3.81	216.6	−1.46	48.58 ± 2.93	46.77	1.81
9	N9	600	150	202.31 ± 3.67	200.43	1.88	51.57 ± 1.52	54.26	−2.69

X_1- CS (mg), X_2- GA (µL), Y_1- Particle size (nm), Y_2- Entrapment efficiency (%) and all values are expressed in Mean ± SD (n = 3).

Table 2. Experimental design with process variables and their levels.

Levels	Independent variables		Dependent variables	
	X_1 CS (mg)	X_2 GA (µl)	Y_1=Particle size (nm)	Y_2=EE (%)
−1	200	50		
0	400	100	Goal to minimize	Goal to maximize
+ 1	600	150		

variables viz., particle size (PS) and entrapment efficiency (EE) were studied.

Determination of particle size and polydispersity index (PDI)

The PS and PDI of the developed nanoparticles were assessed using a Zetasizer (Nano ZS, Malvern Instruments Ltd., Worcestershire, WR14 1XZ, United Kingdom). Millipore water was used to properly dilute each sample and the refractive index was adjusted to 1.33. The temperature at which the analysis was performed was 25ºC [19].

Entrapment efficiency

EE of the CS-VLD-NPs was determined through a centrifugation technique. These samples were centrifuged for 30 minutes at 4°C at 20,000 rpm (KUBOTA 7,000, Japan). The supernatant was collected, and the samples were diluted as needed with phosphate buffer at pH 7.4. These samples were then analyzed at 208 nm using a UV spectrophotometer (Shimadzu 1,900, Japan) [20,21]. The % EE was subsequently calculated using the following formula:

$$\% \text{ EE} = \frac{\text{Amount of drug added} - \text{ unentrapped drug}}{\text{Amount of drug added}} \times 100 \quad (1)$$

FTIR spectroscopy

The interactions between Vildagliptin and Chitosan were investigated, and the structural alterations that resulted from the conjugation of CS-VLD NPs were verified by using an FTIR spectrophotometer (Shimadzu DRS 8,000 IR Affinity-1, Japan), the FTIR spectra of VLD, CS, and CS-VLD NPs were captured. The objective of this investigation was to evaluate the stability of the drug and its interactions with the polymer [22].

Transmission electron microscopy (TEM)

A 0.5 µl sample was collected and diluted using 4 ml of purified water. A diluted sample of 0.2 µl was transferred and coated on a 200-mesh cu-carbon grid. It was then let to dry at room temperature and negatively stained with a 2% solution of phosphotungustic acid. TEM samples were examined at 100 kV using a TECNAI G2 SPIRIT BIOTWIN, MINNESOTA (Make: FEI) [23].

***In vitro* drug release study**

A dialysis bag was used for the *in vitro* drug release study for formulations N3, N6, and N9. In order to investigate the release of VLD, pre-treated dialysis bags (MW of 12 KDa) were filled with CS-VLD-NPs containing 10 mg of VLD, and both ends were sealed. These dialysis bags were immersed in a beaker containing 250 ml of phosphate buffer solution (pH 7.4). A thermostat was used to maintain a 37°C temperature, and the apparatus was set up on a magnetic stirrer with a 100 rpm setting. For up to 24 hours, a 2 ml sample was removed, and a new phosphate buffer solution was added at different intervals.

Spectrophotometric examination of the samples was performed at 208 nm [24].

Kinetics study

Fitting data from *in vitro* releases into several kinetic models, such as the first order, zero order, Korsmeyer-Peppas, and Higuchi models, in order to develop an understanding of the drug release mechanism. The coefficient of correlation (R^2) was used for each model to evaluate the degree to which it fit [25].

Stability study

The CS-VLD-optimized batch (N6) was subjected to a stability study. They were kept for three months in three distinct amber-colored glass bottles that were well sealed. Following the recommendations of the International Council for Harmonization, stability testing of the nanoparticles was conducted at 25°C ± 2°C and 65% relative humidity. Over a 3-month period with a 1-month sampling interval, PS, PDI, and % EE were determined [26].

RESULTS AND DISCUSSION

Optimization of CS-VLD NPs

The CS-VLD NPs were optimized utilizing the two variables and three levels using DoEs software (Design Expert 13). The desolvation method was used to produce CS-VLD NPs, which were then cross-linked with GA. Precipitation and coacervation are two mechanisms involved in the production of nanoparticles. In order to determine the effect of independent factors (X_1, and X_2) on dependent variables (Y_1 and Y_2), a 3^2 RSM was employed. To investigate the effects of an independent variable, Figures 1a and 2a of 2D counter plots and Figures 1b and 2b of 3D response surface graphs were constructed. To investigate the mathematical relationship between independent and dependent variables, counterplots and polynomial equations were constructed. The linear model's correlation coefficients (R^2) values for the responses from Y_1 and Y_2 were 0.9981 and 0.892, respectively, and are presented in Table 3. The ANOVA models for Y_1 and Y_2 are presented in Table 4. The responses for particle size (Y_1) and EE (Y_2) were computed using the following equations:

$$\text{Particle size } (Y_1) = 174.72 + 41.88\ X_1 - 16.17\ X_2 \quad (2)$$

$$\text{EE } (Y_2) = 42.38667 + 7.49000\ X_1 + 4.38000\ X_2. \quad (3)$$

When analyzing the relationship between particle size (Y_1) and the concentration of CS (X_1), it is evident from the positive integer that as the concentration of the polymer increases, the PS also increases. This outcome was expected because higher polymer concentrations lead to an increase in bulk, resulting in larger PSs. Furthermore, the negative integer for X_2 (the amount of GA) shows the negative effect of the cross-linking agent on PS.

With increasing concentrations of the cross-linking agent, there is a hindrance to the further swelling of the polymer, as it tightly holds the polymeric chains. This effect leads to a decrease in PS. The effect is more prominent for X_1 as compared to X_2 which is visible through the integer values (41.88 *vs.* 16.17). In the case of EE, both the variables (X_1 and X_2) have a synergistic effect, which is witnessed through their positive integers in Eqs. 2 and 3. Furthermore, the effect of polymer concentration is more as compared to cross linking agent, this is due to higher polymer concentrations generally lead to increased viscosity during the nanoparticle formation process, which can result in larger PSs and more densely packed polymer matrices. The glutaraldehyde crosslinking of the particle-matrix results in a drop in the isoelectric point of the nanoparticles; however, no discernible effect of the crosslinking conditions on the final PS was detected [27]. The regression analysis of the results obtained has shown that the data fit a linear model for both responses within the study domain space, with R^2 values of0.9981 and 0.892 for Y_1 and Y_2, respectively. ANOVA study has shown the significance of the model with $p < 0.0001$ (for Y_1) and $p < 0.0013$ for Y_2.

Characterization of nanoparticles

PS and PDI

PS and PDI values for all the nanoformulations have been found in the range between 118.24 ± 2.26 nm to 232.84 ± 6.79 nm and from 0.24 ± 0.025 to 0.39 ± 0.037, respectively. Figure 1 represents the 2D and 3D response surface plots for PS. The slopes of the line are indicative of the magnitude of the effect, while the directions of the line are indicative of the positive or negative impact of independent variables on dependent variables. The higher slope of factor A (concentration of CS) indicates its profound effect on PS as compared to factor B (amount of GA). PS increased as CS concentration increased; this could be due to strong intermolecular or intramolecular hydrogen bonds between CS molecules which may cause the nanoparticles to aggregate resulting in a large PS [28,29]. As the degree of cross-linking increased, a rigid matrix formed, enabling for a slight decrease in PS [10]. The PS heterogeneity in NPs was measured using PDI, which shows that the size distribution is narrow. A lower PDI value is highly desirable for the formulations that need a uniform size distribution [30].

Entrapment efficiency

The EE of the CS-VLD NPs was found in the range between 26.45 ± 3.61 and 51.57% ± 1.52% as presented in Table 1. The influence of the VLD to CS ratio on the EE was predicted by the 3D counter-plot (Fig. 2b) using data from the Design-Expert software. EE was shown to increase with increasing CS concentration; finding may be explained by the fact that the increased concentrations of CS offer more capacity to hold drugs. With an increase in polymer concentration up to 400 mg Chitosan (N6), the EE of Chitosan nanoparticles increased. The EE did not significantly increase beyond this concentration, which may be due to the complete saturation of available sites for the entrapment of the drug [31]. However, there has also been a little increase in the EE observed in nanoparticles with an increase in the cross-linking extent. This could be the result of a high crosslink density, which could stop drug particles from leaking out as the nanoparticles are being formed [10].

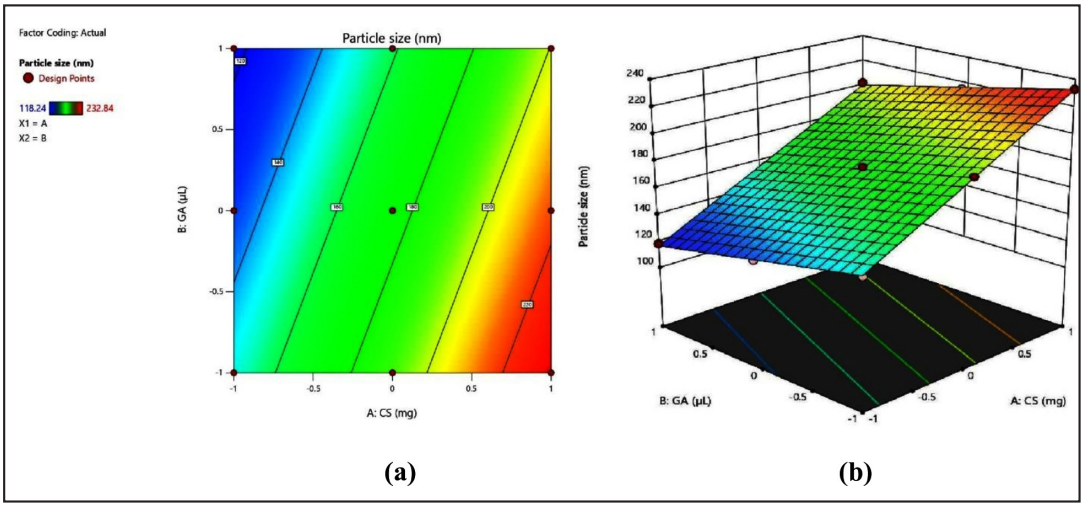

Figure 1. (a) 2D contour plot and (b) 3D response surface plot of PS.

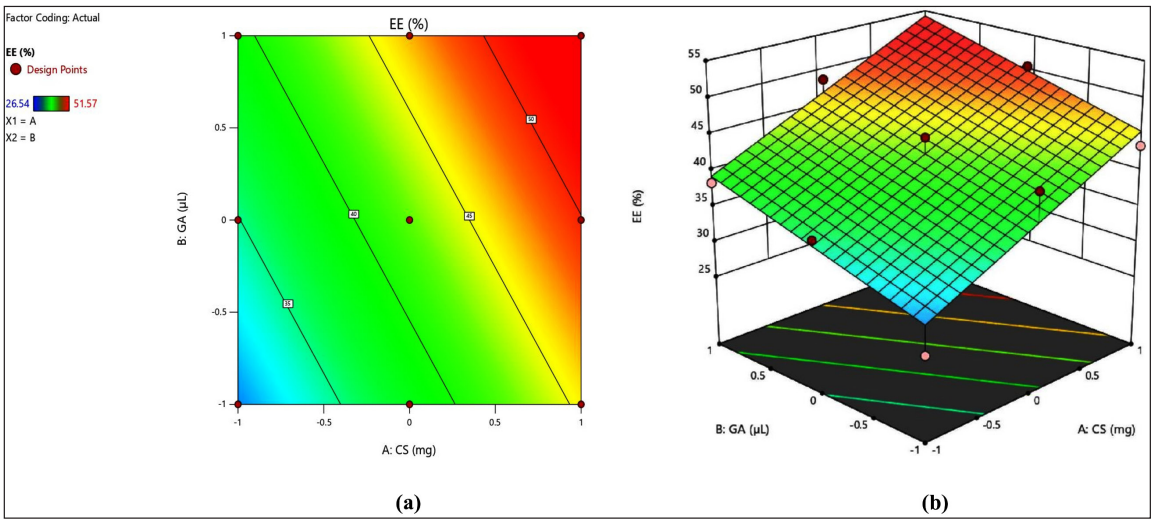

Figure 2. a) 2D contour plot and (b) 3D response surface plot of % EE.

FTIR spectroscopy

The FTIR spectra of (a) VLD, (b) Chitosan, and (c) CS-VLD-NPs are displayed in Figure 3a. Characteristic peaks in the VLD spectrum are seen at 3,492 cm−1 and 2,915 cm−1 (exhibiting O–H and N–H stretching vibrations), 2,125 cm−1 (C≡N stretching), 1,659 cm−1 (amide C=O), and 1,253 cm−1 (C–N stretching). In Figure 3b, we can also observe the infrared spectrum of Chitosan. It is possible to attribute the absorption bands at around 2,869 cm−1 to C-H asymmetric stretching. The bands at about 1,550 cm−1 (C=O stretching of amide I) and 1,350 cm−1 (C-N stretching of amide III), respectively, proved the presence of residual N-acetyl groups. The bands at approximately 1,400 and 1,300 cm−1, respectively, confirmed the CH_2 bending and CH_3 symmetrical deformations. It is possible to explain the absorption band at 1,150 cm−1 to the asymmetric stretching of the C-O-C bridge. The bands corresponding to C-O stretching are located at 1,050 and 1,032 cm−1 [32]. In Figure 3c, The FTIR analysis of CS-VLD nanoparticles shows that the characteristic peaks of both Chitosan and the drug (VLD) are retained without significant shifts or new peaks. This indicates that the drug is physically encapsulated within the Chitosan polymer matrix without strong chemical interactions, ensuring compatibility and preserving the drug's efficacy. The presence of broad bands around 3,400–3,500 cm^{-1}, consistent with O-H and N-H stretching, further supports the conclusion that the functional groups remain intact, confirming that the polymer and drug do not chemically interact significantly.

Transmission electron microscopy

The shape of optimized nanoparticles (N6) has been examined using High-Resolution TEM, and its TEM image is shown in Figure 4. The spherical-shaped nanoparticles that appeared as individual moieties were seen in the TEM investigation.

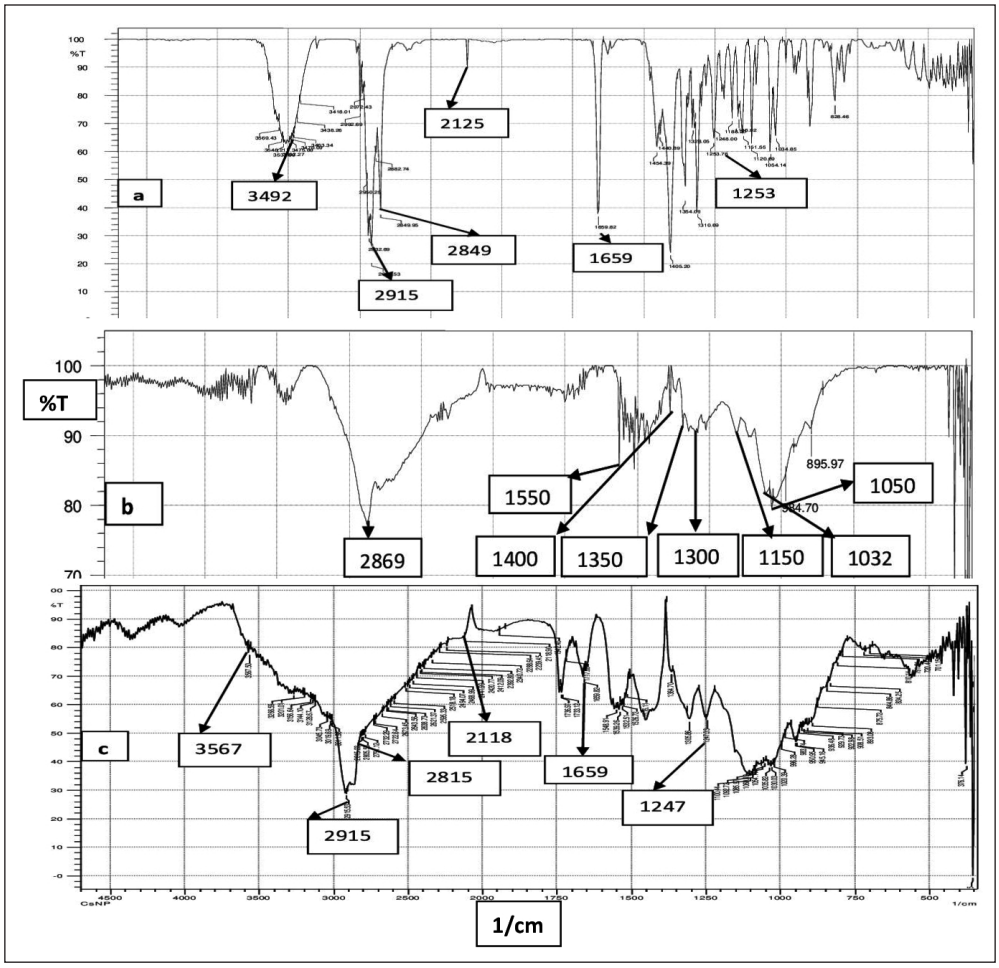

Figure 3. FTIR spectra of (a) VLD, (b) Chitosan, and (c) CS VLD-NPs.

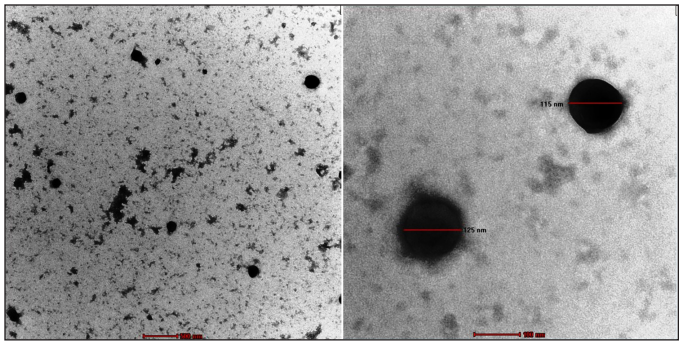

Figure 4. TEM image of optimized CS-VLD NPs.

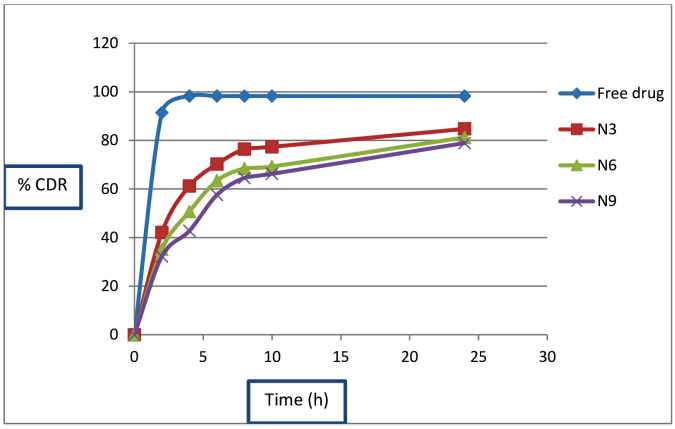

Figure 5. *In vitro* drug release profile of formulation N3, N6 and N9.

In vitro drug release study

Drug release from CS-VLD NPs N3, N6, and N9 was studied by *in vitro* dialysis bag method for 24 hours. The cumulative drug release (%CDR) of pure VLD, N3, N6, and N9 CS-VLD NPs is shown in Figure 5. Over a period of 24 hours, all 3 batches of CS-VLD NPs showed a constant delayed release behavior. About 55%–70% of the drug was released by the nanoparticles in the first 6 hours, followed by 78%–84% in the next 24 hours. The free drug solution exhibited a rapid release profile, with >90% of the drug being released within just 2 hours. Prolonged drug release in the phosphate buffer pH 7.4 was observed. The release of VLD from the nanoparticles started very rapidly in the initial phase which slowed down

Table 3. Summary of results of regression analysis for responses Y_1 and Y_2.

Models	R^2	Adjusted R^2	Predicted R^2	Std dev.	Press	Remarks
Response Y_1 Particle size						
Linear	0.9,981	0.9,974	0.9,957	1.97	51.67	Suggested
2FI	0.9,981	0.9,969	0.9,918	2.16	99.82	
Quadratic	0.9,981	0.995	0.9,807	2.76	233.71	
Cubic	0.9,992	0.9,939	0.8,602	3.05	1,693.53	Aliased
Response Y_2 EE						
Linear	0.892	0.856	0.7,265	3.02	138.47	Suggested
2FI	0.8,989	0.8,382	0.3,876	3.2	310.12	
Quadratic	0.9,788	0.9,436	0.803	1.89	99.74	
Cubic	0.9,872	0.8,973	−1.3,403	2.55	1,185.08	Aliased

Table 4. ANOVA models for Y_1 and Y_2.

Response Y_1: Particle size						
Source	**Sum of Squares**	**df**	**Mean Square**	**F-value**	**p-value**	**Remarks**
Model	12,092.61	2	6,046.31	1,552.79	<0.0001	significant
A-CS	10,524.44	1	10,524.44	2,702.86	<0.0001	
B-GA	1,568.17	1	1,568.17	402.73	<0.0001	
Response Y_2: EE						
Model	451.71	2	225.85	24.78	0.0013	significant
A-CS	336.6	1	336.6	36.94	0.0009	
B-GA	115.11	1	115.11	12.63	0.012	

Table 5. List of the drug release mechanisms.

	N3	N6	N9
Zero order	0.496	0.589	0.639
First order	0.718	0.799	0.834
Higuchi	0.821	0.880	0.912
Korsmeyer-Peppas	0.596	0.628	0.650

Table 6. Stability study of optimized CS-VLD NPs.

Stability parameter	Test period			
	0 month	1 month	2 months	3 months
Particle size (nm)	155.18 ± 3.09	156.2 ± 2.74	158.06 ± 1.46	159.83 ± 0.77
PDI	0.32 ± 0.06	0.34 ± 0.01	0.33 ± 0.02	0.35 ± 0.02
% EE	50.45 ± 1.56	47.29 ± 2.40	48.94 ± 2.24	46.88 ± 0.80

afterward. The drug that has remained on the surface may dissolve quickly in the first fast-release phase. The drug that has been entrapped is dissolved in the following phase when the release medium penetrates nanoparticles [10].

Kinetics study

The release data were subjected to fitting into various kinetic models to estimate the drug release kinetics. The drug release mechanism for N3, N6, and N9 batches are presented in Table 5. According to the kinetic release data of the N3, N6, and N9 formulations, the release characteristic was revealed by the regression coefficient value (R^2) which being highest for the Higuchi model (R^2 = 0.821 0.880 0.912 for N3, N6, and N9, respectively). The Higuchi model describes drug release from a matrix system, primarily focusing on diffusion as the controlling mechanism, which occurs one-dimensionally from the matrix into the surrounding medium [33].

Stability study

For optimized CS-VLD NPs (N6), stability tests were carried out with PS, PDI, and %EE as the main parameters. The stability study results are presented in Table 6. The PS, PDI, and %EE of an optimized formulation (N6) did not significantly alter throughout the course of a 3-month accelerated stability testing, indicating the formulations were stable.

CONCLUSION

In the present investigation, a simple desolvation method was adopted to prepare CS-VLD NPs. The nanoparticle optimization process was successfully carried out using the QbD technique. Based on QbD technique, the optimized formulation for making CS-VLD NPs can be achieved with 400 mg of Chitosan and 150 µl of glutaraldehyde in formulation N6, which shows minimum PS (155.18 ± 3.09 nm) and maximum EE (50.45% ± 1.56%). The formulation's monodispersity is further supported by relatively low PDI (0.32 ± 0.06) and TEM investigations. Since nanoparticles address the issue of frequent VLD dosing for effective diabetes therapy, the observation of a

progressive release of VLD over a 24-hour period suggests the potential use of nanoparticles. Thus, the current investigation demonstrates that optimized CS-VLD NPs may provide improved therapeutic efficacy and sustained drug action, thereby enhancing patient outcomes and treatment adherence, in contrast to conventional drug delivery.

AUTHOR CONTRIBUTIONS

All authors made substantial contributions to conception and design, acquisition of data, or analysis and interpretation of data; took part in drafting the article or revising it critically for important intellectual content; agreed to submit to the current journal; gave final approval of the version to be published; and agree to be accountable for all aspects of the work. All the authors are eligible to be an author as per the International Committee of Medical Journal Editors (ICMJE) requirements/guidelines.

FINANCIAL SUPPORT

There is no funding to report.

CONFLICTS OF INTEREST

The authors report no financial or any other conflicts of interest in this work.

ETHICAL APPROVALS

This study does not involve experiments on animals or human subjects.

DATA AVAILABILITY

All data generated and analyzed are included in this research article.

PUBLISHER'S NOTE

This journal remains neutral with regard to jurisdictional claims in published institutional affiliation.

REFERENCES

1. Tyagi R, Waheed A, Kumar N, Mujeeb M, Naved T, Khan MR, *et al*. *In-vitro* and *ex-vivo* antidiabetic, and antioxidant activities of Box-Behnken design optimized Solanum xanthocarpum extract loaded niosomes. Saudi Pharm J. 2023;31(10):1–12. doi: https://doi.org/10.1016/j.jsps.2023.101785
2. Skelin M, Rupnik M, Cencič A. Pancreatic beta cell lines and their applications in diabetes mellitus research. ALTEX. 2010;27(2):105–13. doi: https://doi.org/10.14573/altex.2010.2.105
3. Odei Addo F, Shegokar R, Müller RH, Levendal RA, Frost C. Nanoformulation of *Leonotis leonurus* to improve its bioavailability as a potential antidiabetic drug. 3 Biotech. 2017;7:1–9. doi: https://doi.org/10.1007%2Fs13205-017-0986-0
4. Gudise V, Chowdhury B, Manjappa AS. Antidiabetic and antihyperlipidemic effects of *Argyreia pierreana* and *Matelea denticulata*: higher activity of the micellar nanoformulation over the crude extract. J Tradit Complement Med. 2021;11(3):259–67. doi: https://doi.org/10.1016/j.
5. Fayyaz S, Ahmed D, Khalid S, Khan SN, Shah MR, Choudhary MI. Synthesis of vildagliptin conjugated metal nanoparticles for type II diabetes control: targeting the DPP-IV enzyme. New J Chem. 2020;44(47):20853–60. doi: https://doi.org/10.1039/D0NJ04202A
6. Kushwaha RN, Srivastava R, Mishra A, Rawat AK, Srivastava AK, Haq W, *et al.* Design, synthesis, biological screening, and molecular docking studies of piperazine-derived constrained inhibitors of DPP-IV for the treatment of type 2 diabetes. Chem Biol Drug Des. 2015;85(4):439–46. doi: https://doi.org/10.1111/cbdd.12426
7. Nagaraja SH, Al-Dhubiab BE, Tekade RK, Venugopala KN, Ghorpade RV, Meravanige G, *et al*. Novel preparation and effective delivery of mucoadeshive nanoparticles containing anti-diabetic drug. Indian J Pharm Edu Res. 2019;53(2):43–9. doi: https://doi.org/10.5530/ijper.53.2s.47
8. Sreeharsha N, Rajpoot K, Tekade M, Kalyane D, Nair AB, Venugopala KN, *et al*. Development of metronidazole loaded chitosan nanoparticles using QbD approach—A novel and potential antibacterial formulation. Pharmaceutics. 2020;12(10):1–22. doi: http://dx.doi.org/10.3390/pharmaceutics12100920
9. Hamed R, Jodeh S, Hanbali G, Safi Z, Berisha A, Xhaxhiu K, *et al*. Eco-friendly synthesis and characterization of double-crossed link 3D graphene oxide functionalized with chitosan for adsorption of sulfamethazine from aqueous solution: experimental and DFT calculations. Front Environ Sci. 2022;10:1–19. doi: https://doi.org/10.3389/fenvs.2022.930693
10. Agnihotri SA, Aminabhavi TM. Chitosan nanoparticles for prolonged delivery of timolol maleate. Drug Dev Ind Pharm. 2007;33(11):1254–62. doi: https://doi.org/10.1080/03639040701384942
11. Aggarwal D, Kaur IP. Improved pharmacodynamics of timolol maleate from a mucoadhesive niosomal ophthalmic drug delivery system. Int J Pharm. 2005;290(1-2):155–9. doi: https://doi.org/10.1016/j.ijpharm.2004.10.026
12. De Campos AM, Sánchez A, Alonso MJ. Chitosan nanoparticles: a new vehicle for the improvement of the delivery of drugs to the ocular surface. Application to cyclosporin A. Int J Pharm. 2001;224(1-2):159–68. doi: https://doi.org/10.1016/S0378-5173(01)00760-8
13. De Campos AM, Sánchez A, Gref R, Calvo P, Alonso MJ. The effect of a PEG versus a chitosan coating on the interaction of drug colloidal carriers with the ocular mucosa. Eur J Pharm Sci. 2003;20(1):73–81. doi: https://doi.org/10.1016/S0928-0987(03)00178-7
14. Mohammed MA, Syeda JY, Wasan KM, Wasan EK. An overview of chitosan nanoparticles and its application in non-parenteral drug delivery. Pharmaceutics. 2017;9(4):1–26. doi: https://doi.org/10.3390/pharmaceutics9040053
15. Xu X, Khan MA, Burgess DJ. A quality by design (QbD) case study on liposomes containing hydrophilic API: I. Formulation, processing design and risk assessment. Int J Pharm. 2011;419(1-2):52–9. doi: https://doi.org/10.1016/j.ijpharm.2011.07.012
16. Shah B, Khunt D, Bhatt H, Misra M, Padh H. Intranasal delivery of venlafaxine loaded nanostructured lipid carrier: risk assessment and QbD based optimization. J Drug Deliv Technol. 2016;33:37–50. doi: https://doi.org/10.1016/j.jddst.2016.03.008
17. Li Z, Cho BR, Melloy BJ. Quality by design studies on multi-response pharmaceuticalformulation modeling and optimization. J Pharm Innov. 2013;8(1):28–44. doi: https://doi.org/10.1007/s12247-012-9145-7
18. Mishra V, Thakur S, Patil A, Shukla A. Quality by design (QbD) approaches in current pharmaceutical set-up. Expert Opin Drug Deliv. 2018;15(8):737–58. doi: https://doi.org/10.1080/17425247.2018.1504768
19. Praveen A, Aqil M, Imam SS, Ahad A, Moolakkadath T, Ahmad FJ. Lamotrigine encapsulated intra-nasal nanoliposome formulation for epilepsy treatment: formulation design, characterization and nasal toxicity study. Colloids Surf B Biointerfaces. 2019;174:553–62. doi: https://doi.org/10.1016/j.colsurfb.2018.11.025
20. Moolakkadath T, Aqil M, Ahad A, Imam SS, Iqbal B, Sultana Y, *et al*. Development of transethosomes formulation for dermal fisetin delivery: box–Behnken design, optimization, *in vitro* skin penetration, vesicles–skin interaction and dermatokinetic studies. Artif Cells NanomedBiotechnol. 2018;46(2):755–65. doi: https://doi.org/10.1080/21691401.2018.1469025
21. Shirsath NR, Goswami AK. Vildagliptin-loaded gellan gum mucoadhesive beads for sustained drug delivery: design, optimisation

and evaluation. Mat Technol. 2021;36(11):647–59. doi: https://doi.org/10.1080/10667857.2020.1786783
22. Abolhasani A, Heidari F, Abolhasani H. Development and characterization of chitosan nanoparticles containing an indanonic tricyclic spiroisoxazoline derivative using ion-gelation method: an *in vitro* study. Drug Dev Ind Pharm. 2020;46(10):1604–12. doi: https://doi.org/10.1080/03639045.2020.1811304
23. Malatesta M. Transmission electron microscopy for nanomedicine: novel applications for long-established techniques. Eur J Histochem. 2016;60(4):8–12. doi: https://doi:10.4081/ejh.2016.2751
24. Wallenwein CM, Nova MV, Janas C, Jablonka L, Gao GF, Thurn M, *et al*. A dialysis-based *in vitro* drug release assay to study dynamics of the drug-protein transfer of temoporfin liposomes. Eur J Pharm Biopharm. 2019;143:44–50. doi: https://doi:10.1016/j.ejpb.2019.08.010
25. Deshmukh RK, Naik JB. Optimization of sustained release aceclofenac microspheres using response surface methodology. Mater Sci Eng C. 2015;48:197–204. doi: http://dx.doi.org/10.1016/j.msec.2014.12.008
26. Hernandez Patlan D, Solis Cruz B, Cano Vega MA, Beyssac E, Garrait G, Hernandez Velasco X, *et al*. Development of chitosan and alginate nanocapsules to increase the solubility, permeability and stability of curcumin. J Pharm Innov. 2019;14:132–40. doi: https://doi.org/10.1007/s12247-018-9341-1
27. Mehravar R, Jahanshahi M, Saghatoleslami N. Fabrication and evaluation of human serum albumin (HSA) nanoparticles for drug delivery application. Int J Nanosci. 2009;8(03):319–22. doi: https://doi.org/10.1142/S0219581X09006080
28. Aktas Y, Andrieux K, Alonso MJ, Calvo P, Gursoy RN, Couvreur P, *et al*. Preparation and *in vitro* evaluation of chitosan nanoparticles containing a caspase inhibitor. Int J Pharm 2005;298:378–83. doi: https://doi.org/10.1016/j.ijpharm.2005.03.027
29. Banerjee T, Mitra S, Singh AK, Sharma RK, Maitra A. Preparation, characterization and biodistribution of ultrafine chitosan nanoparticles. Int J Pharm 2002;243:93–105. doi: 10.1016/s0378-5173(02)00267-3
30. Avadi MR, Sadeghi AM, Mohammadpour N, Abedin S, Atyabi F, Dinarvand R, *et al*. Preparation and characterization of insulin nanoparticles using chitosan and Arabic gum with ionic gelation method. Nanomed: Nanotechnol Biol Med. 2010;6(1):58 63. doi: https://doi.org/10.1016/j.nano.2009.04.007
31. Nagarajana E, Shanmugasundarama P, Ravichandirana V, Vijayalakshmia A, Senthilnathanb B, Masilamanib K. Development and evaluation of chitosan based polymeric nanoparticles of an antiulcer drug lansoprazole. J Appl Pharm Sci. 2015;5(4):20–5. doi: https://doi.org/10.7324/JAPS.2015.50404
32. Waghulde MR. Naik JB. Comparative study of encapsulated vildagliptin microparticles producedby spray drying and solvent evaporation technique. Dry Technol. 2017;35:1644–55. doi: https://doi.org/10.1080/07373937.2016.1273230
33. Jain D, Banerjee R. Comparison of ciprofloxacin hydrochloride-loaded protein, lipid, and chitosan nanoparticles for drug delivery. J Biomed Mater Res B Appl Biomater. 2008;86(1):105–12. doi: https://doi.org/10.1002/jbm.b.30994

How to cite this article:
Ammanage AS, Mastiholimath VS. Quality by design approach assisted development and optimization of Chitosan-vildagliptin nanoparticles using a simple desolvation technique. J Appl Pharm Sci. 2025;15(03):174–182.